Prepublished copy

Nature Environment & Pollution Technology

This is a peer-reviewed prepublished version of the paper

*Type of the Paper (Original Research)*

# Enhanced LULC Classification Using CNNs with Transfer Learning and Fine-Tuning: A Regional Study

**Mahendra H. N.[1], Basavaraju, N. M.[2]†, Ravi, P.[3], Pushpalatha, V.[4] and Mallikarjunaswamy, S.[5]**

[1, 2,5]Department of Electronics and Communication Engineering, JSS Academy of Technical Education (Affiliated to Visvesvaraya Technological University, Belagavi), Bengaluru-560060, Karnataka, India

[3]Department of Information Science and Engineering, Maharaja Institute of Technology Mysore (Affiliated to Visvesvaraya Technological University, Belagavi), Mandya-571477, Karnataka, India

[4] Department of Information Science and Engineering, JSS Academy of Technical Education (Affiliated to Visvesvaraya Technological University, Belagavi), Bengaluru-560060, Karnataka, India

†Corresponding author: Basavaraju N. M.; basavarajunm@jssateb.ac.in

| | |
|---|---|
| Key Words | Remote sensing, Deep learning, Convolutional neural networks, Land use and cover, Transfer learning and Fine-tuning |
| DOI | https://doi.org/10.46488/NEPT.2026.v25i02.B4375 (DOI will be active only after the final publication of the paper) |
| Citation for the Paper | Mahendra H. N., Basavaraju, N. M., Ravi, P., Pushpalatha, V. and Mallikarjunaswamy, S. 2026. Enhanced LULC classification using CNNs with transfer learning and fine-tuning: A regional study. *Nature Environment and Pollution Technology*, 25(2), B4375. https://doi.org/10.46488/NEPT.2026.v25i02.B4375 |

**ABSTRACT**

In recent days, due to the high population and rapid urbanization, we have challenged several problems related to environmental degradation and climate change. Therefore, Land Use Land Cover (LULC) classification is important in providing accurate and timely information about natural and land resources. Traditional methods for the classification of satellite imagery face several challenges due to the complexities and variability of the data. In this paper, we proposed a novel approach to enhance LULC classification using deep learning-based convolutional neural networks with extraction of features, transfer learning, and fine-tuning. The proposed work first designs convolutional neural networks from scratch to capture spatial features from multispectral resolution satellite imagery covering the study area of Mysuru taluk, Karnataka State, India. Transfer learning is then applied to adapt the pre-trained CNN model to the LULC classification. Furthermore, fine-tuning is employed to fine-tune the adapted CNN model on the target dataset, enabling the model to learn domain-specific features and improve classification performance. The proposed deep learning model performance is demonstrated through experiments on multispectral datasets, where convolutional neural networks, transfer learning, and fine-tuning models provide classification accuracy of 90.41%, 92.50%, and 94.37%, respectively.

## INTRODUCTION

Monitoring changes in land use and land cover (LULC) is vital for understanding the dynamic interaction between human activities and natural ecosystems. Population growth, agricultural expansion, industrialization, urbanization, and climate variability have significantly altered terrestrial landscapes, resulting in challenges related to food security, biodiversity loss, water scarcity, and environmental sustainability (Alhassan, V. et al. 2020; Mozumder et al., 2025). Timely and accurate mapping of LULC is therefore indispensable for urban planning, sustainable development, disaster management, and policy-making. Remote sensing (RS) has emerged as the most efficient tool for LULC studies because it provides repetitive, synoptic, and multispectral coverage of Earth's surface over extensive areas at varying spatial and temporal scales (Carranza-García et al., 2019; Kumar et al., 2021).

Traditional approaches to LULC classification predominantly rely on machine learning (ML) methods such as Maximum Likelihood Classification (MLC), k-Nearest Neighbor (k-NN), Decision Trees (DT), Random Forests (RF), and Support Vector Machines (SVM) (Mahendra H.N et al. 2023a). These classifiers have been widely applied in remote sensing tasks due to their computational efficiency and robust mathematical foundation. However, their performance is constrained by their dependence on hand-crafted spectral, spatial, or textural features that must be manually engineered prior to classification. Such dependency leads to high subjectivity and model bias, while also requiring domain-specific expertise for feature extraction (Balarabe, A.T et al. 2021; K. Ganesha Raj et al. 2021). Furthermore, ML classifiers often fail to achieve high accuracy in heterogeneous landscapes where spectral overlap, high intra-class variability, and mixed pixels are common problems that are especially prominent in medium-resolution imagery. These limitations underscore the need for more flexible and data-driven approaches that can automatically discover representative features from raw imagery (Kumar, S et al., 2021; Mahendra H.N et al. 2023b).

Recent developments in deep learning (DL) have revolutionized computer vision and have shown tremendous promise in the field of remote sensing. Convolutional Neural Networks (CNNs), in particular, have demonstrated their capacity to learn hierarchical spectral–spatial representations from imagery, thereby eliminating the need for handcrafted features. By automatically capturing low-level edge features, mid-level textures, and high-level semantic patterns, CNNs offer a significant advantage in classifying complex and heterogeneous land cover categories (Maggiori et al., 2017; Boyang Li et al., 2020). Their ability to generalize across spectral bands, spatial resolutions, and contextual patterns makes them especially suitable for LULC mapping RS (Gibril, M.B et al. 2017; Geetha, M.A et al. 2021).

However, the successful training of CNNs requires very large labeled datasets, which are often unavailable in remote sensing applications (Boyang Li et al. 2020). Annotated RS datasets are expensive, time-consuming, and labor-intensive to generate, particularly in developing countries (García-Gutiérrez et al. 2010; Liang H et al. 2016). Additionally, training CNNs from scratch demands substantial computational resources and optimized hyperparameter tuning, which can be prohibitive in many practical settings (Li, B. et al. 2020; Naushad, R. et al. 2021). To overcome these challenges, transfer learning (TL) and fine-tuning (FT) strategies have gained significant attention.

Transfer learning leverages knowledge from pre-trained CNN models developed on large-scale datasets such as ImageNet, enabling re-use of learned filters for new but related tasks in RS (Dewangkoro, H.I et al. 2021; Gisela Häufel et al. 2018). The generic edge and texture features from early CNN layers remain useful across domains, reducing the need for large labeled datasets. Fine-tuning goes one step further by retraining the deeper network layers to adapt to domain-specific characteristics of RS data, ensuring improved generalization and accuracy (Naushad et al., 2021; Shabbir et al., 2021). Such approaches strike a balance between computational feasibility and classification performance, making them highly relevant for RS-based LULC applications.

The efficiency of TL and FT has been demonstrated across multiple RS domains including urban expansion monitoring, vegetation type classification, crop yield estimation, and disaster damage assessment. Studies have reported that CNN-based TL models consistently outperform traditional classifiers and even outperform CNNs trained from scratch in limited-data scenarios. Moreover, advanced CNN architectures such as VGGNet, ResNet, DenseNet, and EfficientNet have introduced innovative scaling mechanisms that improve accuracy while reducing computational complexity. Among these, EfficientNet stands out due to its compound scaling approach, which balances network depth, width, and input resolution, making it highly suitable for large and medium-scale RS applications (E. Maggiori et al. 2017; Mahendra, H.N et al. 2023c).

Despite this progress, a notable research gap persists: most DL studies in RS prioritize high-resolution imagery such as Sentinel-2 (10 m) and Landsat-8 (30 m), while medium-resolution imagery from LISS-III sensor (23.5 m) remains largely underexplored. LISS-III provides cost-effective, regionally relevant data that is widely utilized in India for agricultural monitoring, forest assessment, hydrology, and urban planning. However, applications of advanced CNN-based DL methods to LISS-III imagery are still limited, with existing studies focusing more on conventional ML techniques or unsupervised classification approaches (Pushpalatha et al., 2025). This underrepresentation is striking, given the operational importance of LISS-III in India's remote sensing programs and its widespread use for regional-scale resource management.

Motivated by this gap, the present study undertakes a systematic exploration of DL strategies for LULC classification using IRS LISS-III imagery of Mysuru Taluk, Karnataka, India. Specifically, we investigate and compare three CNN-based strategies. The choice of EfficientNetB7 is motivated by its demonstrated efficiency in balancing accuracy with computational demands, making it a strong candidate for medium-resolution RS applications.

To ensure a comprehensive evaluation, we also benchmark these DL models against traditional ML classifiers such as SVM, RF, DT, k-NN, and MLC using the same LISS-III dataset. Our study ensures a fair and controlled comparison by applying all models on the same dataset under identical conditions. This approach not only strengthens the credibility of performance assessment but also provides practical insights into the suitability of different classifiers for medium-resolution RS applications. The key contributions of this study include:

1. We employ the region-specific LISS-III dataset of Mysuru Taluk, Karnataka, which is relatively underexplored in deep learning-based LULC studies, thereby providing insights into a critical region experiencing rapid land-use transitions.
2. We adapt and fine-tune the EfficientNetB7 architecture for multi-class LULC classification, redesigning the dense layer to suit regional data.
3. We present a direct performance comparison between a CNN designed from scratch and transfer learning models, highlighting their trade-offs under limited data availability.

Finally, the outcomes of this study are positioned within the framework of sustainable development and regional planning, emphasizing the applied significance of our findings beyond methodological comparisons.

## 1. RELATED WORKS

In the literature, several researchers explored the use of deep learning techniques, including CNN, transfer learning, and fine-tuning, to enhance LULC classification. Weng et al. (2017) proposed a method that combines CNN and ELM to improve classification performance. Zhu et al. (2020) focused on the high-resolution satellite image classification for land cover classes with a high total accuracy of 89.6% through the use of an improved SMOTE algorithm for sample augmentation. Douass et al. (2022) applied a transfer learning approach, retraining a pre-trained Resnet18 model to classify aerial images of the Tangier region. Alem et al. (2020) provided a comprehensive review of methods in deep learning for the classification of LULC, highlighting the use of CNN models in this field.

Agarwal et al. (2022) proposed an innovative approach to LULC classification by using satellite imagery and deep learning techniques. This method utilizes high-resolution satellite images to automatically extract the optimal feature for land cover classification. Similarly, Xia et al. (2022) developed a deep learning model specifically designed for LULC classification, employing a seven-layer CNN to achieve effective results. Uba (2019) also explored the use of techniques of deep learning for LULC classification, demonstrating how these algorithms can effectively process very high spatial resolution images to automate LULC identification. In another study, Kalantar et al. (2022) presented a deep ensemble learning framework for LULC classification using hyperspectral PRISMA imagery, focusing on extracting critical information to enhance classification accuracy.

Nijhawan et al. (2018) introduced a forward-looking framework of deep learning for the classification of LULC using remote sensing data and provides better performance as compared to existing methods. Similarly, Song et al. (2019) presented a novel approach utilizing a 1D CNN for the classification of LULC in satellite images, where the application of the CNN to each pixel in the spectral domain significantly improved classification accuracy. Liu et al. (2020) proposed a LULC classification method that integrates CNN with a digital surface model, and remote sensing data, achieving an impressive overall accuracy of 95.57%. Yang et al. (2019)

developed a CNN-based approach for LULC classification, where the inclusion of an infrared band and data provided better classification results compared to traditional RGB images.

Yang et al. (2021) introduced a deep-learning framework for the consistent classification of land-use objects within geospatial databases. This approach is based on CNNs, to predict land use across multiple hierarchical levels simultaneously and demonstrates superior performance compared to existing methods. Kussul et al. (2017) developed a model of deep learning for classifying crop and land cover types using satellite data. This architecture, utilizing an ensemble of CNNs, significantly outperformed models based on MLPs. Patel et al. (2022) proposed a multi-level feature extraction technique for automated land cover classification, integrating LSTM networks and deep CNNs. This model exceeded the performance of benchmark pre-trained CNN models.

Rao et al. (2022) presented an advanced algorithm based on deep learning for classifying LULC using satellite imagery. This approach utilized the DeepLabv3 model, a semantic segmentation framework employing atrous convolution to capture multi-scale contexts. This is achieved by adopting multiple atrous rates in a cascading or parallel manner to accurately determine the scale of land segments. Yang et al. (2019) proposed a highly efficient and accurate deep learning-based method for large-scale land-use mapping, utilizing a deep convolutional neural network to achieve superior results. Bergado et al. (2020) introduced a land-use classification method using deep multitask networks, which outperformed other classifiers by at least 30% in the average F1-score. Fahmi et al. (2022) focused on patch-based land cover classification and demonstrated that ResNet-50 achieved the highest validation accuracy for this task. Weng et al. (2018) developed a CNN-based land-use scene classification model that incorporates a constrained extreme learning machine (CNN-CELM). This model not only enhances generalization capabilities but also reduces training time compared to other state-of-the-art methods. Collectively, these studies highlight the significant potential of deep learning in enhancing the accuracy and efficiency of LULC classification.

## 2. MATERIALS AND METHODS

### 2.1 Objectives

The primary goal of this study is to improve LULC classification accuracy. In order to accomplish this goal, the research has delineated the following objectives:

1. To design CNNs from scratch to extract high-level features from satellite imagery for LULC classification.
2. To apply the transfer learning DL model to improve the performance of LULC classification.
3. To further enhance the classification accuracy and optimize model performance through the process of fine-tuning the DL model.

### 2.2 Study Area

In this research work, Mysuru taluk, Karnataka State, India is identified as a study area as shown in Fig. 1. Mysuru taluk, located in the southern part of Karnataka, India, is renowned for its rich cultural heritage, historical significance, and serene landscapes. The taluk encompasses a diverse array of topographies, from lush green forests to fertile plains, interspersed with villages and urban developments. Serving as the administrative hub of the region, Mysuru taluk boasts a vibrant blend of tradition and modernity, with its iconic Mysore Palace standing tall as a testament to its royal past. The area is not only a place for tourists seeking a glimpse of its regal architecture and captivating festivals but also a hub for academic pursuits with institutions like the University of Mysore contributing to its intellectual vibrancy. Additionally, the taluk's agrarian landscape fosters a thriving agricultural sector, with crops like sugarcane, paddy, and silk serving as economic mainstays.

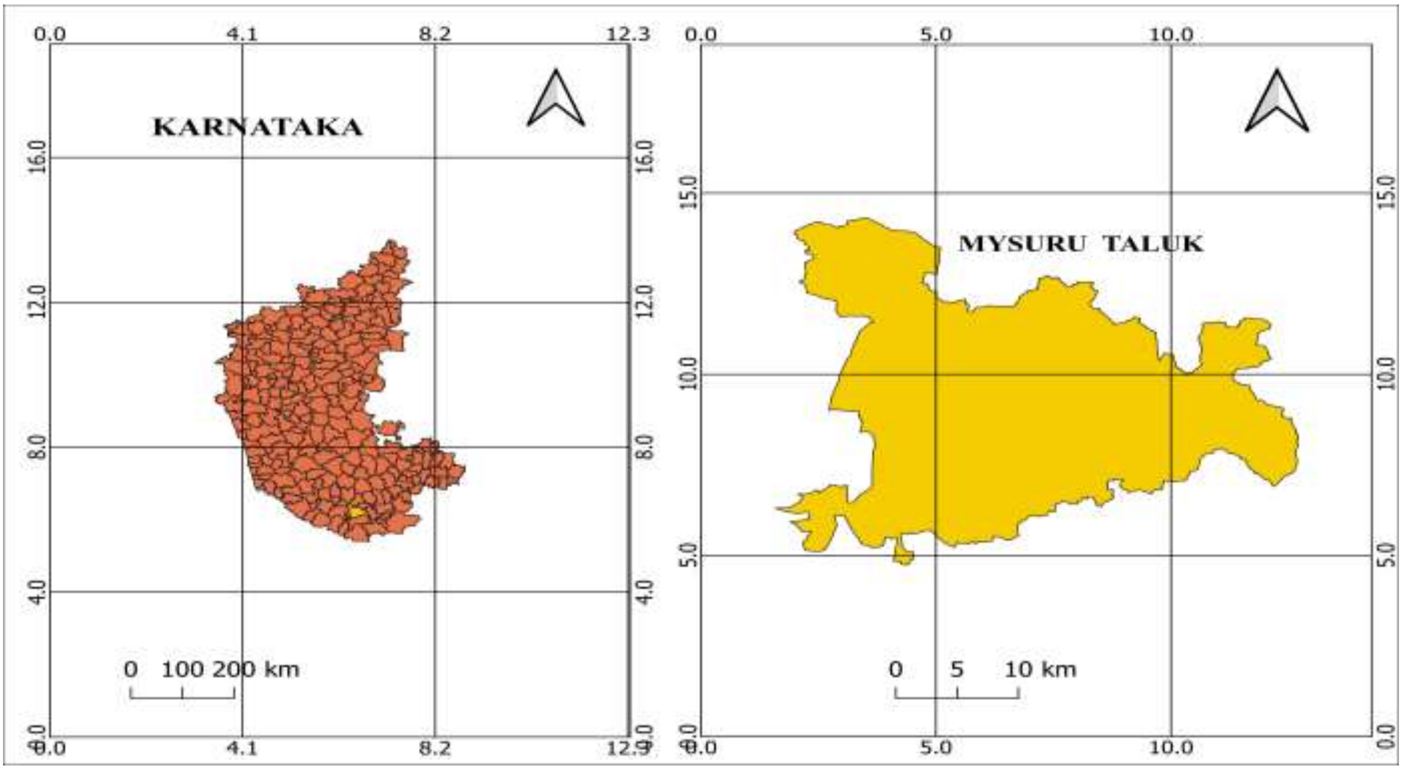


**Fig. 1.** Study area of Mysuru taluk

**2.3 Dataset and Tools**

In this research work, Resourcesat-1 satellite, Linear Imaging Self-Scanning Sensor-III (LISS-III) sensor data of the year 2019 covering the Mysuru taluk is downloaded from ISRO Bhuvan portal and used for modeling the CNN, transfer learning, and fine-tuning. The study area was obtained in six image patches, which were merged and cropped to the exact Mysuru taluk boundary using the QGIS tool**.** The Resourcesat-1 satellite, equipped with the LISS-III sensor, provides invaluable data for various applications including land use planning, agriculture, forestry, and environmental monitoring. LISS-III captures images with a 23.5-meter spatial resolution in four spectral bands ranging from visible to near-infrared. This high-resolution data enables detailed analysis of land cover changes, vegetation health, and natural resource management over large areas. Its ability to acquire images in multiple spectral bands supports differentiating land cover types and detecting environmental variations, making Resourcesat-1 LISS-III a vital tool for sustainable development and scientific research.

High-level programming languages like Python are useful for creating DL models. Python is an easy-to-use and adaptable programming language that may be used to build a variety of interactive libraries for the many learning and machine learning models. Additional tools that are utilized with Python include MAT LAB R2023b, QGIS, and TensorFlow.

### 2.4 Methodology

The proposed research methodology to enhance the LULC classification accuracy through models such as CNN-feature extraction (CNN--FE), transfer learning, and fine-tuning is shown in Fig. 2. First, a satellite dataset encompassing diverse land cover types and regions covering Mysuru taluk is collected and preprocessed. The study area was obtained in six image patches, which were merged and cropped to the exact Mysuru Taluk boundary using the QGIS tool. The preprocessing step includes data processing such as radiometric and geometric corrections, normalization, and augmentation to ensure a balanced and robust dataset for training the deep learning models. Every dataset was divided into 60% training, 20% validation, and 20% test samples. Additionally, as indicated in Table 1, we set up the DL hyperparameters for the dataset training. After the models were trained and validated using the validation dataset, their performance was evaluated using the test dataset.

Further, a CNN architecture is designed from scratch as a feature extractor to automatically learn discriminative features from the raw input imagery. This CNN architecture is developed to effectively capture the spatial dependencies and hierarchical representations within the input data. Transfer learning is then employed by utilizing pre-trained EfficientNet CNN models. By leveraging the knowledge encoded in these pre-trained models, the network can expedite the learning process and adapt to the specific LULC classification task more efficient transfer learning.

Fine-tuning the DL model involves fine-tuning the pre-trained EfficientNet CNN model on the target LULC dataset. During this process, the weights of the pre-trained model are adjusted through backpropagation while the model is trained on the LULC dataset. This fine-tuning stage allows the network to specialize and refine its learned features according to the degrees of the target task, thereby improving classification performance. Additionally, techniques such as regularization and hyperparameter tuning are employed to optimize the model's generalization capability and performance on unseen data.

Lastly, the trained model is evaluated using various metrics such as overall accuracy, precision, recall, and F1-score using a test dataset. The performance of the proposed DL model is compared with the state-of-the-art methods to assess its effectiveness in enhancing LULC classification accuracy. Additionally, sensitivity analysis is conducted to evaluate the robustness of the model to variations in input data and parameter settings. This comprehensive evaluation provides insights into the strengths and limitations of the proposed methodology and guides future improvements and applications in the field of land use analysis and remote sensing.

**Table 1.** Hyperparameters are used to train the model.

| **Hyperparameters** | **Values** |
|---|---|
| Dropout | 0.25 |
| Loss Function | Cross-entropy |
| Activation Function | ReLU, Sofine-tuning max |
| Epochs | 100 |
| Batch Size | 64 |
| Optimizers | Adam |
| Learning rate | 0.001 |

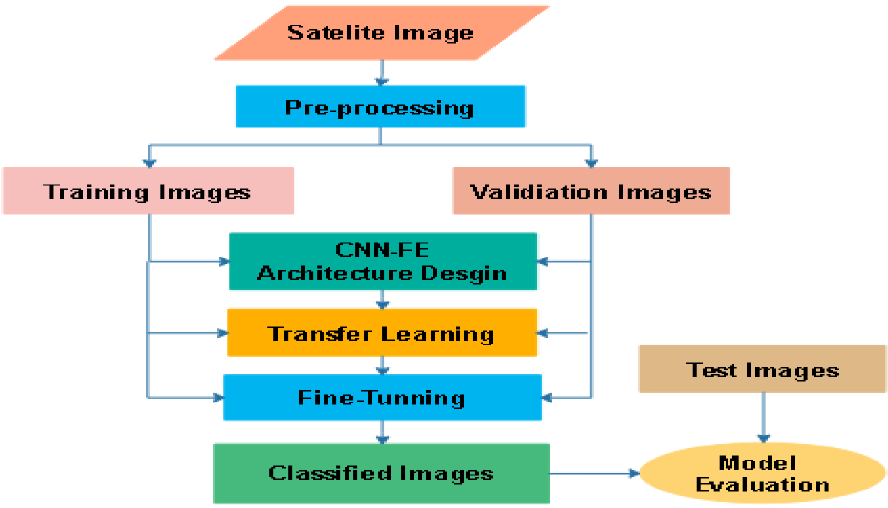


**Fig. 2.** Methodology followed in the research work

## 3. PROPOSED DEEP LEARNING METHODS

### 3.1 Convolutional Neural Networks-Feature Extraction (CNN-FE)

The proposed CNN architecture begins with preprocessing of LISS-III satellite data, where images are downloaded, merged, cropped, and resized to a uniform 224x224x3 dimension. The model's input layer is configured to accept images of this size. The architecture includes eight convolutional layers, each employing various filter sizes to capture diverse features within the image. This multi-scale approach enhances feature extraction capabilities, allowing the network to capture finer details and complex patterns in the satellite data for more accurate analysis as shown in Fig. 3.

The initial convolutional layer utilizes 32 filters of size 1x1 with a stride of 1, allowing the filter to traverse one pixel at a time across the input image. The absence of padding in this layer means the spatial dimensions of the output are reduced. Following this, a second convolutional layer is incorporated, which also employs 32 filters but with a larger 2x2 filter size, maintaining the stride at 1 and similarly applying no padding. This sequential application of convolutional layers allows for the extraction of both fine-grained and slightly more complex spatial features without border augmentation.

A third convolutional layer with 64 filters of size 2x2, a stride of 1, and no padding to capture finer image details. The subsequent, fourth convolutional layer employs 64 filters of size 3x3, also with a stride of 1 and no padding, facilitating the extraction of more complex features. Together, these layers enhance the model's ability to identify intricate patterns within the data. This configuration aims to progressively refine feature extraction, providing a solid foundation for accurate image classification or detection tasks.

Feature extraction is progressively refined across successive convolutional layers, enhancing the network's depth and capturing complex patterns. The fifth convolutional layer uses 128 filters of size 3x3, followed by a sixth layer with 128 filters of size 4x4, both with a stride of 1 and no padding. The seventh and eighth layers further deepen the model, employing 256 filters of sizes 3x3 and 4x4, respectively, also with a stride of 1 and zero padding. This layered architecture aims to capture fine-grained details in the input data, optimizing feature representation for subsequent classification tasks.

In CNN, activation functions are crucial for enabling the network to model complex data patterns. After each convolutional layer, an activation layer is typically applied, with the Rectified Linear Unit (ReLU) being one of the most popular choices. ReLU is computationally efficient and simple, outputting zero for negative inputs and the original value for non-negative inputs. This function's simplicity enhances computational speed and implementation ease. A key advantage of ReLU is its ability to introduce non-linearity into the network, essential for learning intricate data relationships. Without non-linearity, neural networks would behave linearly, regardless of depth, limiting their ability to capture complex patterns. Additionally, ReLU mitigates the vanishing gradient problem, where gradients diminish during backpropagation, especially in deep architectures. These properties make ReLU a preferred activation function in deep learning, enhancing model performance in applications such as LULC classification.

The max pooling layers follow each convolutional layer to reduce the spatial dimensions of feature maps, preserving essential information while enhancing computational efficiency. This down-sampling technique is crucial for tasks like image recognition and structured data analysis. Convolutional layers in CNNs first capture basic features such as edges and textures, which are then refined through pooling layers to detect more complex patterns and objects. Max pooling operates by sliding a fixed-size window across the feature map, selecting the maximum value in each window to summarize key information.

The proposed CNN architecture integrates eight distinct max-pooling layers, each positioned after successive convolutional layers, featuring varied kernel sizes and stride values for optimal spatial reduction of feature maps. The first pooling layer is designed with a kernel size of 2x2 and a stride of 1, while the second employs a 3x3 kernel with a stride of 2. The third and fourth layers share a kernel size of 3x3 but differ in stride values of 2 and 3, respectively. Following these, the fifth and sixth layers utilize 4x4 and 5x5 kernels with stride values of 2. The seventh pooling layer is designed with a 4x4 kernel and a stride of 3, and the eighth layer has a 3x3 kernel with a stride of 5. This tailored configuration enables a controlled reduction in the spatial dimensions of feature maps. For an input feature map of dimensions nh×nw×nc, the output dimensions after max-pooling are defined in Equation (1).

$$(n_h - f + 1)/s * (n_w - f + 1)/s * n_c \text{ ------------ } (1)$$

where,

$n_h$- height of feature map
$n_w$- width of feature map
$n_c$- channel numbers
s- stride length
f – filter size

The proposed CNN, batch normalization is implemented within the CNN architecture to enhance training speed, stability, and overall performance. This layer normalizes layer inputs by scaling activations, ensuring a consistent distribution of features. By mitigating internal covariate shift, batch normalization reduces sensitivity to weight initialization and learning rates, aiding in stable model training. It also minimizes the need for dropout by naturally regularizing the network. Additionally, batch normalization helps smooth the loss landscape across mini-batches, facilitating faster convergence and improved network generalization.

In CNN architecture, three fully connected (FC) layers follow the convolutional and pooling layers to facilitate the mapping of learned features to the output space. These layers contain 1024, 512, and 4 neurons, respectively. Each neuron in the FC layers is connected to every neuron in the preceding layer, allowing the network to capture complex global patterns. This configuration enables effective transformation of feature representations into a structured output. The final layer with 4 neurons corresponds to the target output classes.

In the proposed model, the first FC layer with 1024 neurons extracts a rich set of abstract features from the data. The second FC layer, with 512 neurons, reduces dimensionality to refine these learned features further. The final FC layer with 4 neurons functions as the output layer, facilitating classification. This layered approach ensures a smooth transition from spatial feature extraction by CNN layers to decision-making, enhancing classification accuracy in the targeted tasks.

The objective function layer, as the final layer in a CNN, calculates the error, or loss, between the actual target values and model's predictions. Located after the output layer, this layer uses a designated loss function commonly cross-entropy loss in classification tasks to measure prediction error. This error, represented as a scalar value, quantifies the model's deviation from true outcomes. Feeding this error into backpropagation, the network updates its weights and biases to reduce error in future iterations. The objective function layer thus steers the learning process, guiding the network to enhance its accuracy over time. Cross-entropy loss is particularly suitable for classification tasks, efficiently managing multi-class outputs as shown in equation (2). Through iterative training, this mechanism allows the network to gradually refine its predictions and improve overall performance.

$$L_{soft\ \max loss]} = -\frac{1}{N}\sum_{i=1}^{N}\log\left(\frac{e^{hy_i}}{\sum_{j=1}^{C}e^{h_j}}\right) \quad (2)$$

With $yi \in \{1,2,\ldots\ldots,C\}$

$$h = \{h1, h2, \ldots\ldots, hc)\mathrm{T} \quad (3)$$

In this notation, *yi* represents the true label, C is the total number of classes, and **h** corresponds to the final output of the architecture.

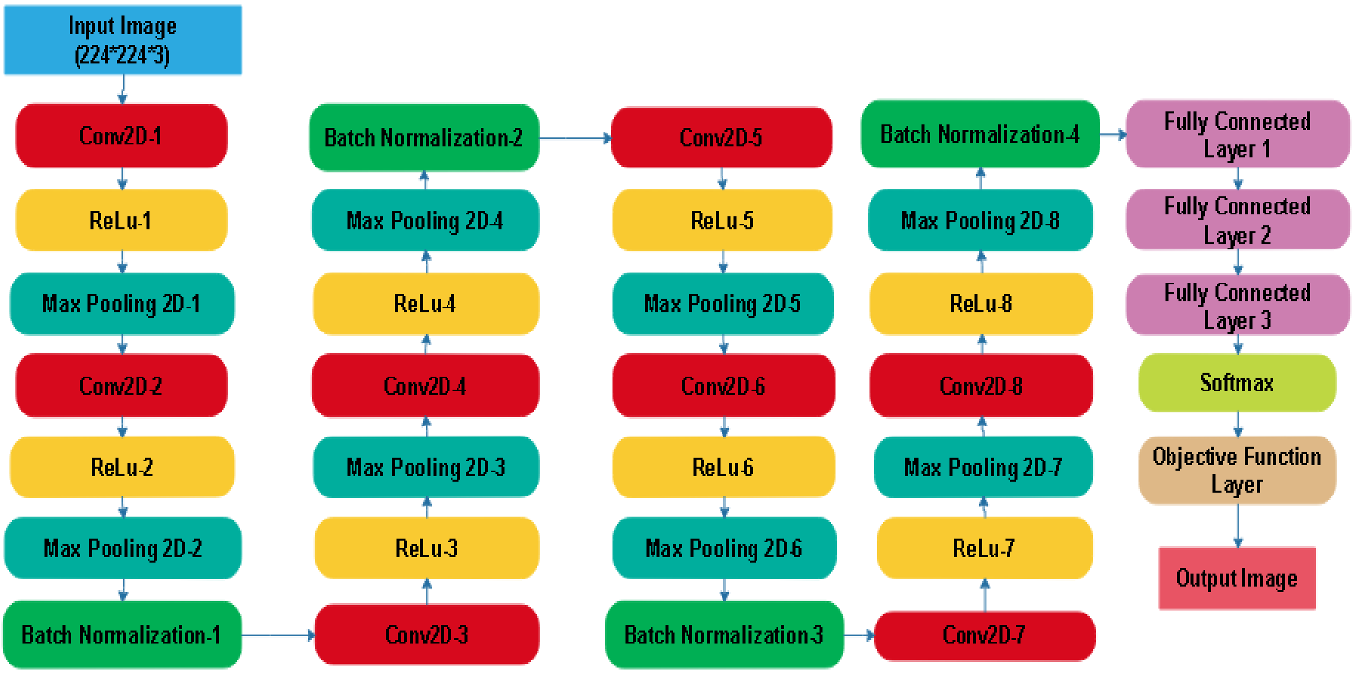


**Fig. 3.** Proposed CNN architecture

### 3.2 Transfer Learning Method

Transfer learning is a powerful technique in machine learning that leverages pre-trained models to improve the performance of LULC classification. In the context of LULC classification, transfer learning is particularly useful due to the vast amount of labeled satellite imagery required for training models from scratch. Instead of starting with an untrained model, a deep learning model pre-trained on a large dataset like EfficienNet can be fine-tuned for LULC classification. This process adapts the learned features from general image classification to the specific patterns found in satellite or aerial imagery, such as vegetation, urban areas, and water bodies.

Transfer learning significantly reduces the computational cost and training time while often improving accuracy, as the model already has a good understanding of visual features like edges, textures, and shapes. Fine-tuning involves adjusting the weights of the last few layers of the model or replacing them entirely with new layers suited to the LULC task. This approach is particularly effective when labeled data is scarce, as it avoids the need for large-scale, labeled training sets typical in remote sensing applications. Transfer learning can also be used with modern architectures like CNNs and is instrumental in improving the efficiency of LULC classification tasks.

### 3.3 Fine-Tuning

Fine-tuning for LULC classification involves adapting a pre-trained deep learning model, usually a CNN, to classify satellite images into specific land cover categories. The process starts with using a model pre-trained on a large dataset, like EfficientNet, to leverage its learned features. Fine-tuning focuses on training only the final layers while keeping the earlier layers frozen, as they have already learned general features such as edges and textures. First, satellite data are used to replace the last classification layer of the model with a new layer that matches the number of LULC classes. During training, the model learns to recognize land cover types such as forests, urban areas, water bodies, and agricultural land. Key techniques include adjusting learning rates, data augmentation, and using transfer learning to speed up the process. This method reduces the need for large datasets and extensive computational resources, making it effective for LULC classification while improving accuracy. Fine-tuning is essential when domain-specific patterns differ from the general features learned in the original dataset.

## 4. RESULTS

The experiments conducted on a laptop computer with an Intel Core i3-6006U CPU running at 2.00GHz and 12 GB of RAM. The MAT LAB R2023b and QGIS tools are used with the Python programming language.

### 4.1 Training and Validation

We used a satellite data set of the Mysuru taluk to assess the deep learning models' performance in LULC classification. Training, validation, and test samples make up 20%, 20%, and 60% of the dataset, respectively. In addition, the model is trained and validated using a training and validation dataset, and its performance is evaluated using a test dataset.

We trained and validated the model during experiments using training and validation datasets once the experimental settings were set. Additionally, test data sets were used to assess the model's performance in terms of accuracy, recall, f1-score, and precision using a confusion matrix. The confusion matrix shows how well the class did based on how accurately or poorly the rows and columns in the intersections are classified. The categorical-cross-entropy loss function was used to calculate the accuracy and errors.

The CCN-FE, transfer learning, and fine-tuning model's training and validation accuracy are shown in Fig.4, Fig. 5, and Fig. 6 (on the left), respectively, which is anticipated to increase in epoch increments. Fig. 4, Fig. 5, and Fig. 6 (on the right) show the losses of training and validation of the CCN-FE, transfer learning, and fine-tuning model respectively, which are anticipated to decrease in epoch increments.

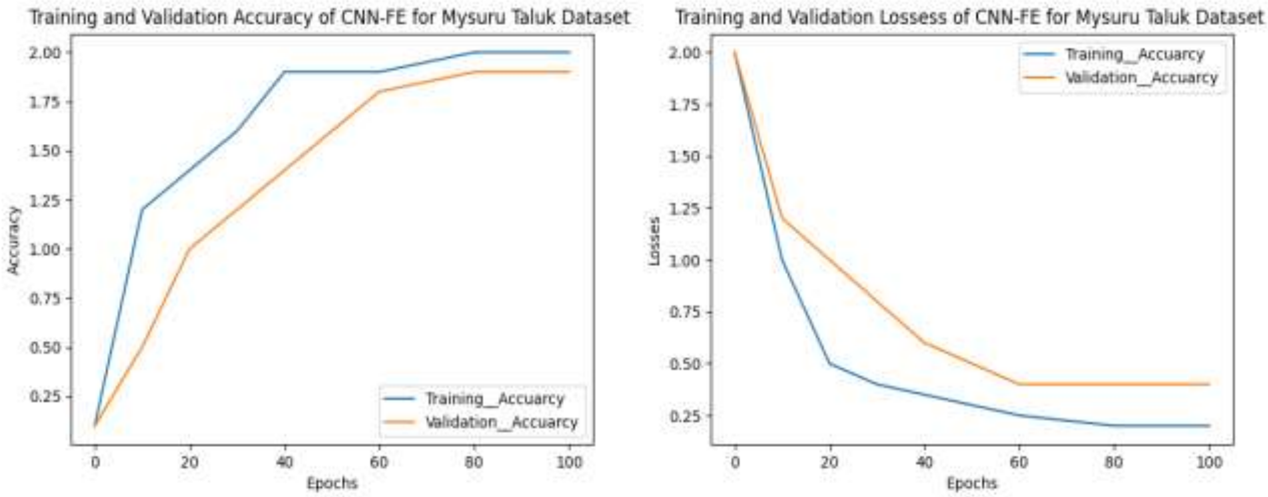


**Fig. 4.** CNN-FE training and validation accuracy

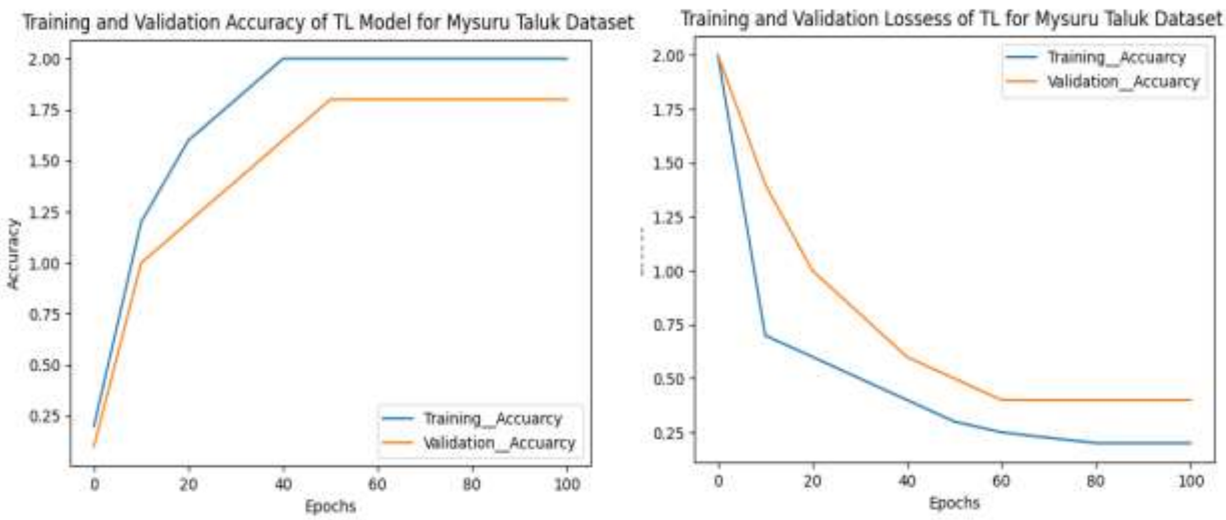


**Fig. 5.** Training and validation accuracy of transfer learning

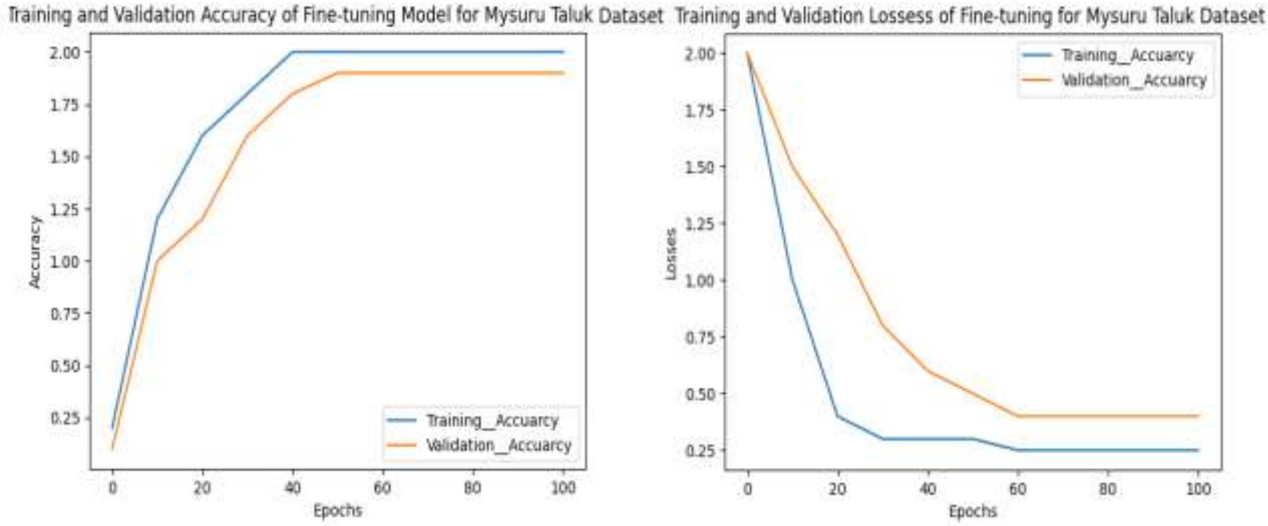


**Fig. 6.** Training and validation accuracy of Fine-tuning

### 4.2 LULC Classification and Assessment

LULC classification is performed using all three of the trained DL models CNN-FE, transfer learning, and fine-tuning on LISS-III sensor data of the year 2019 of Mysuru Taluk. The CNN-FE, transfer learning, and fine-tuning classified maps are depicted in Fig. 7, Fig. 8, and Fig. 9, respectively. Throughout the study region, the primary LULC classes are built-up areas, agricultural land, water bodies, forests, and other landscape features. The LULC area for every class has been assessed for each of the three classed maps. Each land class's area in sq. km and its percentage of the total area occupied by all classes are listed in Table 2. The Mysuru Taluk covers a total geographical area of 797 sq. km. Built-up areas were identified to cover approximately 200.42 sq. km, accounting for 25.14% of the total area using the CNN-FE model. Similarly, transfer learning and fine-tuning models identified built-up areas to cover 202.24 sq. km (25.37%) and 201.69 sq. km (25.30%) respectively. Agriculture land constituted the majority of the area under study, covering 473.60 sq. km (59.42%) with CNN-FE, 473.06 sq. km (59.36%) with transfer learning, and 474.12 sq. km (59.48%) with fine-tuning model.

Water bodies were found to cover 36.82 sq. km (4.61%) using CNN-FE, 35.28 sq. km (4.42%) using transfer learning, and 36.35 sq. km (4.56%) using the fine-tuning model. Forested areas accounted for 61.61 sq. km (7.73%), 63.15 sq. km (7.92%), and 62.19 sq. km (7.80%) with CNN-FE, transfer learning, and fine-tuning models respectively. Waste land types collectively covered 24.55 sq. km (3.08%), 23.46 sq. km (2.94%), and 22.65 sq. km (2.84%) with CNN-FE, transfer learning, and fine-tuning models respectively. These results indicate consistency across the three models in delineating land cover classes, with slight variations in area estimations.

**Table 2.** Mysuru taluk LULC assessment of CNN-FE, transfer learning, and fine-tuning

| | CNN-FE | Transfer Learning | Fine-tuning |
|---|---|---|---|

| Class Name | | | | | | |
|---|---|---|---|---|---|---|
| | Area (in Sq. km) | % Area | Area (in sq. km) | % Area | Area (in Sq. km) | % Area |
| Built-up | 200.42 | 25.14 | 202.24 | 25.37 | 201.69 | 25.30 |
| Agriculture land | 473.60 | 59.42 | 473.06 | 59.36 | 474.12 | 59.48 |
| Water bodies | 36.82 | 4.61 | 35.28 | 4.42 | 36.35 | 4.56 |
| Forest | 61.61 | 7.73 | 63.15 | 7.92 | 62.19 | 7.80 |
| Waste land | 24.55 | 3.08 | 23.46 | 2.94 | 22.65 | 2.84 |

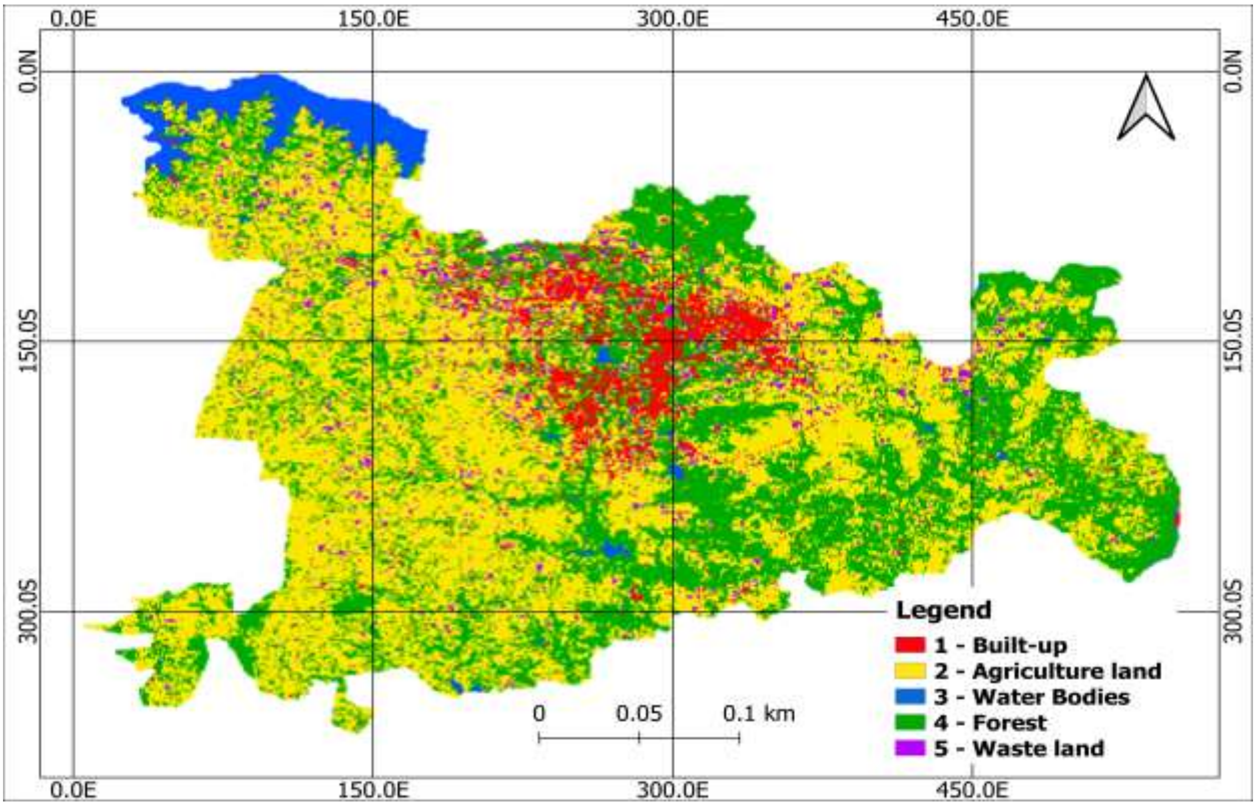


**Fig. 7.** Classified map of Mysuru taluk using CNN-FE

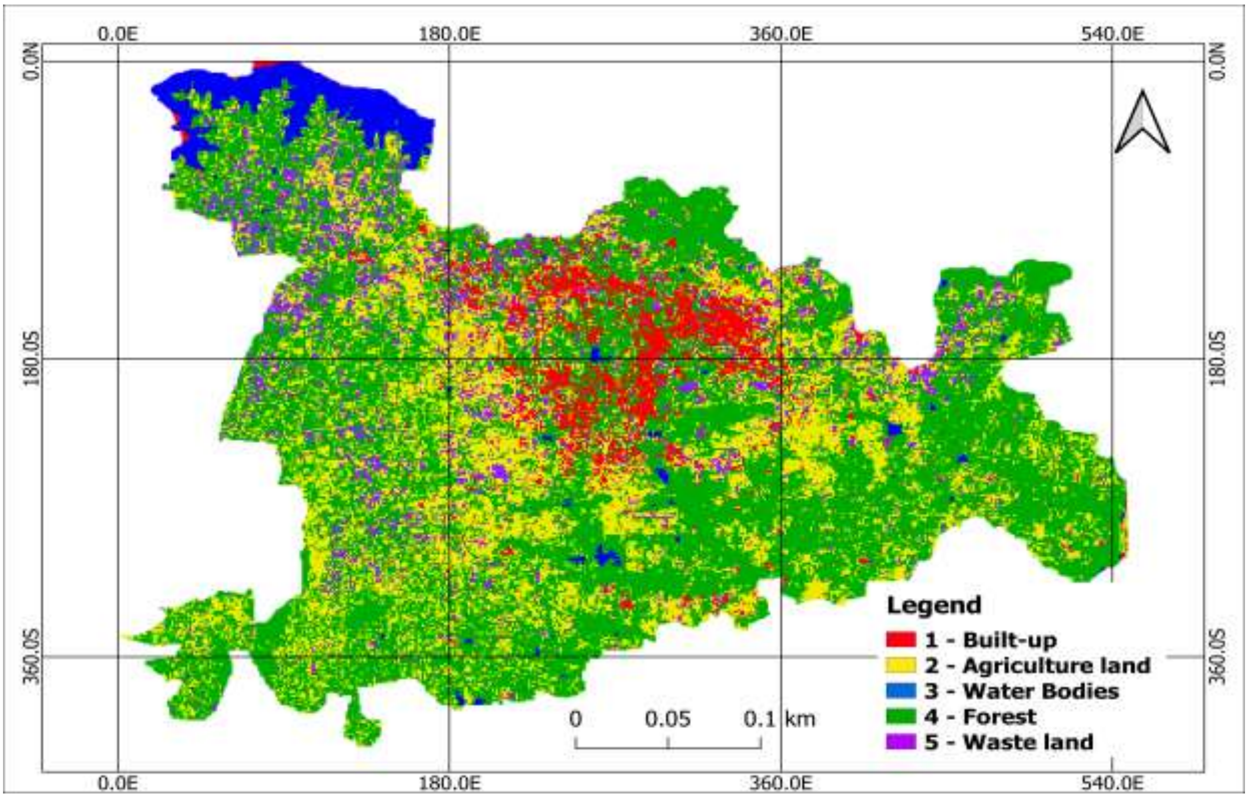


**Fig. 8.** Classified map of Mysuru taluk using transfer learning

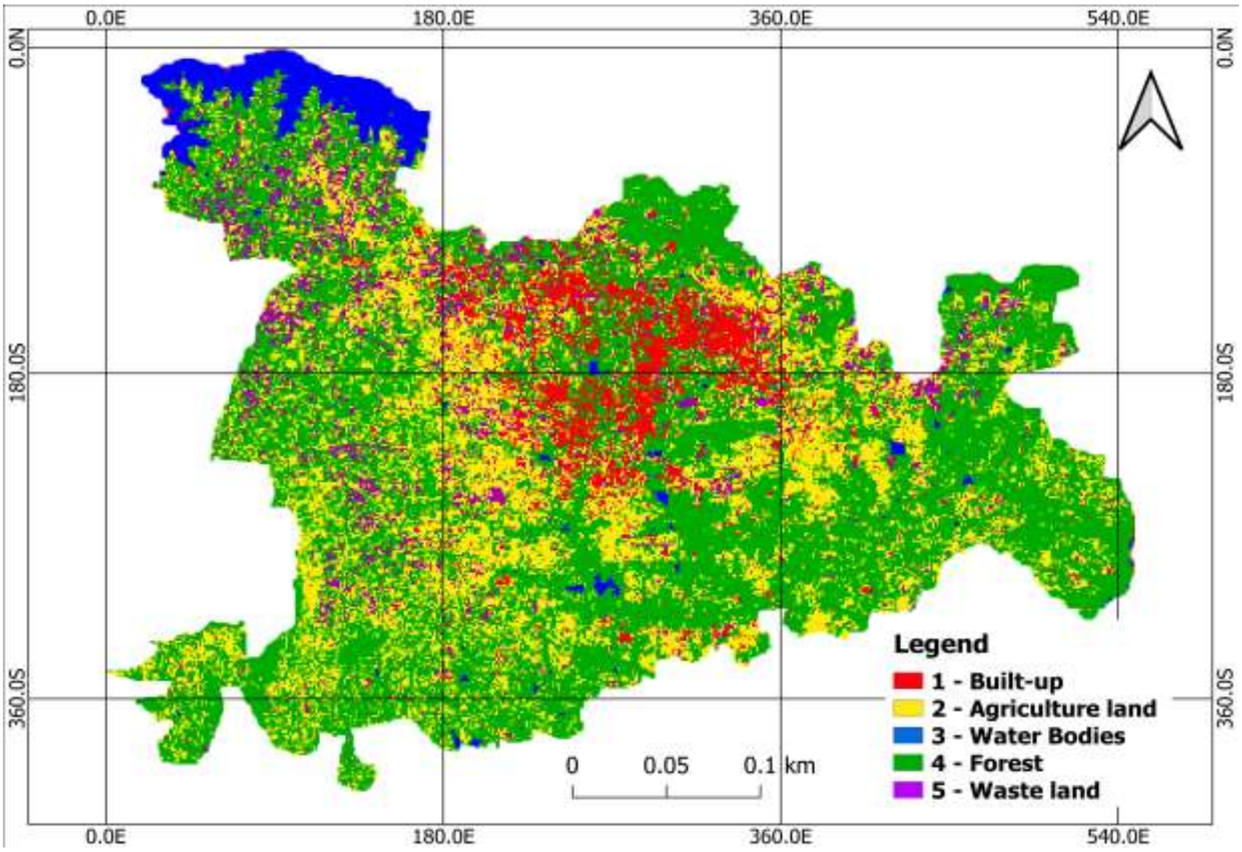


**Fig. 9.** Classified map of Mysuru taluk using Fine-tuning

### 4.3 Performance Analysis of DL Models

We use 480 test data sets to assess the performance of each DL model. In addition to the accuracy measure, the kappa value, precision, recall, and F1 score are used to assess each class's performance. The CNN-FE, transfer learning, and fine-tuning performance are shown in Tables 3, 4, and 5, respectively. The F1-score, which generalizes the average performance of the constructed DL models and the performance of each class, is calculated using the harmonic mean of accuracy and recall metrics. The F1-score also performs at the highest level in that class if recall and precision do as well. Conversely, if accuracy or recall yield zero performance results, the F1-score has zero performance, indicating that the model is not making any predictions.

The F1-score metric has a 100% score in the built-up class in the transfer learning model (Table 4), the agriculture land class in CNN-FE (Table 3), and the fine-tuning model (Table 5), according to the classification results. The accuracy and loss metrics are also employed to illustrate the suitability of the DL models; the CNN-FE, transfer learning, and fine-tuning models are shown in Figures 4, 5, and 6, respectively. Figures 4, 5, and 6 illustrate how the training accuracy (represented by a blue color curve) and validation accuracy (represented by a red color curve) rise linearly with the number of epochs. We reduced errors in the model's performance by using the cross-entropy loss function.

**Table 3.** CNN-FE classification performances

| Classes of LULC | Precision | Recall | F1-Score |
|---|---|---|---|
| Built-up | 0.95 | 0.95 | 0.90 |
| Agriculture land | 1.00 | 1.00 | 1.00 |
| Water Bodies | 0.73 | 0.95 | 0.84 |
| Forest | 0.86 | 0.95 | 0.90 |
| Waste land | 0.91 | 0.75 | 0.83 |

**Table 4.** Transfer learning classification performance

| Classes of LULC | Precision | Recall | F1-Score |
|---|---|---|---|
| Built-up | 1.00 | 1.00 | 1.00 |
| Agriculture land | 1.00 | 0.95 | 0.96 |
| Water Bodies | 0.69 | 0.90 | 0.78 |
| Forest | 0.82 | 0.90 | 0.86 |
| Waste land | 0.95 | 0.90 | 0.92 |

**Table 5**. Fine-tuning classification performance

| Classes of LULC | Precision | Recall | F1-Score |
|---|---|---|---|
| Built-up | 1.00 | 0.90 | 0.98 |
| Agriculture land | 1.00 | 1.00 | 1.00 |
| Water Bodies | 0.76 | 0.95 | 0.83 |
| Forest | 0.87 | 0.88 | 0.90 |
| Waste land | 0.94 | 1.00 | 0.95 |

# 5. DISCUSSION

## 6.1 Confusion Matrix

In this research work, we applied deep learning models for classification of LCLU on satellite images. Several measuring metrics have been used to evaluate DL models' performance. Initially, we employed a confusion matrix to assess class performances and overall accuracy of each DL model along with recalls, f1-score, and precision. Similar to the F1-score, the confusion matrix measure shows improved class performance in the majority of classes. Table 6, Table 7, and Table 8 show the confusion matrix constructed for DL models of CNN-FE, transfer learning, and fine-tuning respectively. As seen in Table 6, Table 7, and Table 8 confusion matrix takes into account each true labeled class in a row and predicted labeled class in columns. The diagonal intersection's probability score indicated which classed classes were correct. On the other hand, it is anticipated that the results in the remaining rows and columns will belong to incorrect classes.

Table 6, the confusion matrix analysis for the CNN-FE model shows its performance across various classes. The expected class is shown by each column, and the true class is represented by each row. For each class, the diagonal elements represent correctly classified examples, whereas the off-diagonal elements represent incorrectly classified occurrences. By examining these values, we can discern the model's strengths and weaknesses in classifying different categories. Notably, high values along the diagonal indicate robust classification performance, whereas off-diagonal values highlight areas for improvement or potential sources of confusion. Such insights can guide further refinement of the CNN-FE model architecture or dataset preprocessing to enhance classification accuracy.

Table 7, shows the confusion matrix analysis for the transfer learning model and provides a detailed overview of its classification performance. Leveraging pre-trained weights from a different task or domain, the transfer learning model adapts its knowledge to the target classification problem. Similar to the CNN-FE analysis, the confusion matrix delineates correct and erroneous classifications across different classes. Discrepancies between true and predicted labels are evident in off-diagonal elements. These findings explain the effectiveness of transfer learning in leveraging prior knowledge for improved classification while identifying areas where fine-tuning may be beneficial to bolster performance further.

Finally, in Table 8, the confusion matrix analysis for the fine-tuning model provides further insights into its classification performance. Fine-tuning involves training a pre-trained model on a new dataset with a small learning rate, allowing it to adapt to the details of the target task while retaining the knowledge gained from the original training. By examining the distribution of correct and incorrect classifications across classes, we can gauge the effectiveness of fine-tuning in improving model performance. This analysis helps in identifying any disparities between predicted and actual class labels, guiding subsequent adjustments to the fine-tuning process to enhance classification accuracy and overall model efficiency.

The performance results of DL models in LULC classification are shown in Table 9. The study's findings demonstrate that the proposed DL models were able to adapt and gain improved remote sensing capabilities. The CNN-FE that was built from scratch performs substantially less than transfer learning and fine-tuning model performances.

The experiment results demonstrate a progressive enhancement in accuracy among three DL models. Initially, the CNN-FE achieves a respectable accuracy of 90.41%, indicating the effectiveness of feature extraction in refining input data representations. Transfer learning further boosts performance, and provides a notably improved accuracy of 92.50%. Finally, fine-tuning provides the highest accuracy of 94.37%, showcasing the substantial benefits of fine-tuning to adapt a pre-trained model to a specific task, enabling it to learn task-specific patterns effectively. These results emphasize the importance of methodological refinement and model optimization in achieving superior performance in CNN-based classification tasks.

**Table 6** Confusion matrix of CNN-FE

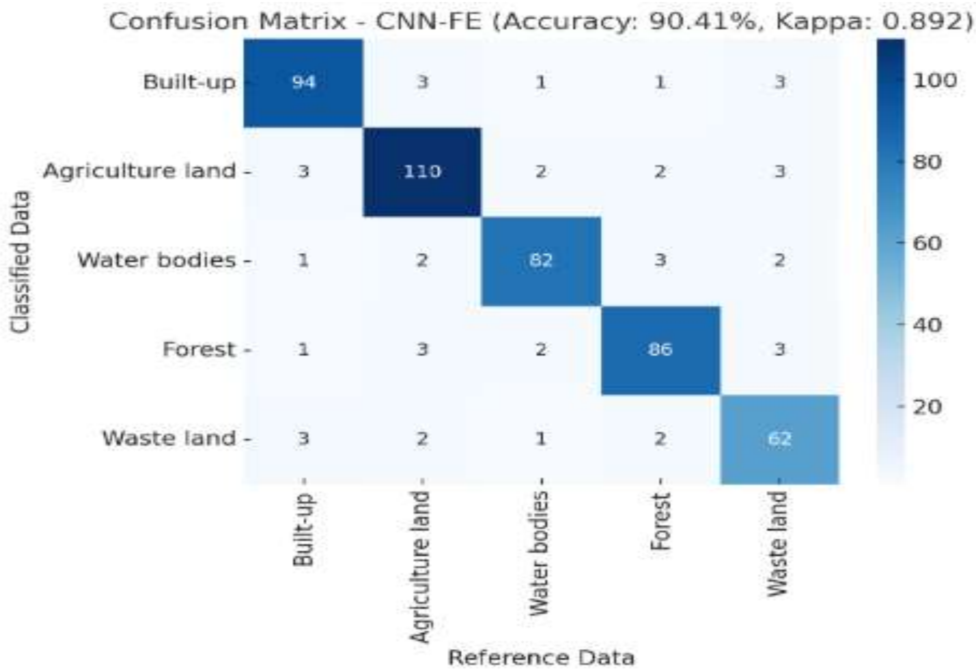

**Table 7** Confusion matrix of transfer learning

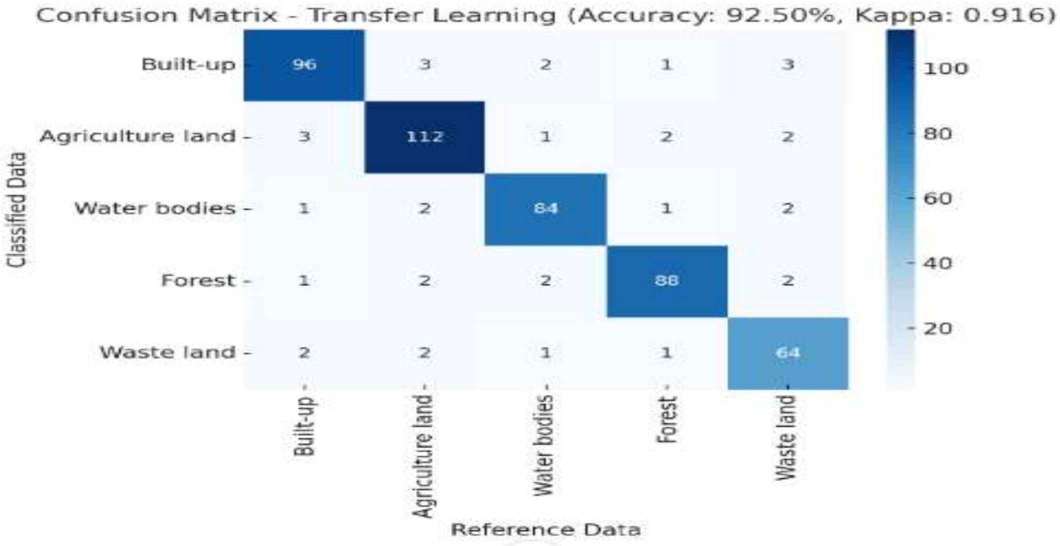


**Table 8.** Confusion matrix of fine-tuning

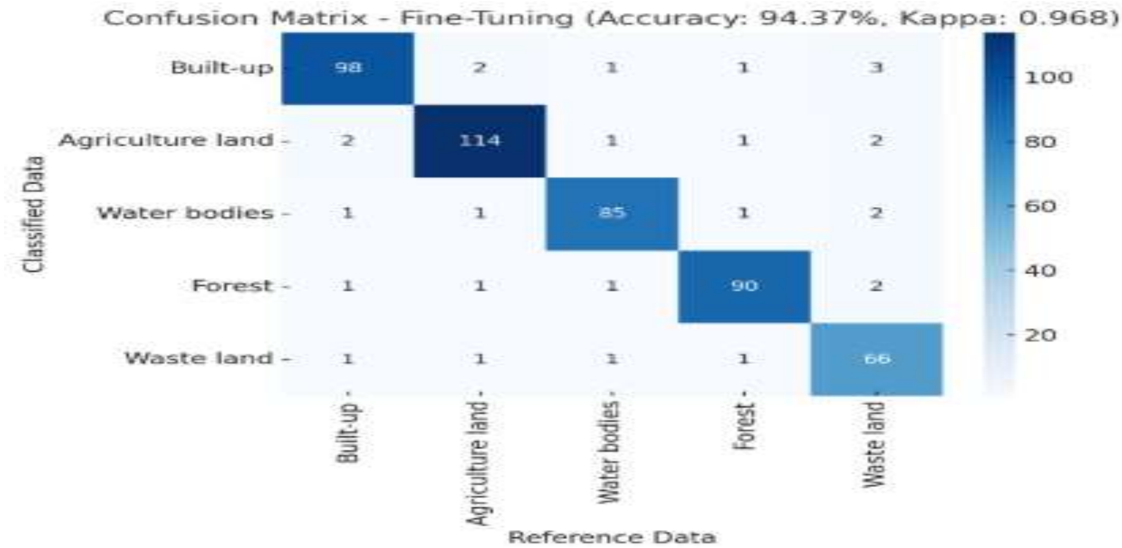


**Table 9.** DL models performance analysis using various performance matrices on satellite data

| DL Models | Performance Metrics | | | | | Training Time (s) | Testing Time (s) |
|---|---|---|---|---|---|---|---|
| | Precision (%) | Recall (%) | F1-Score (%) | Accuracy (%) | Kappa value | | |
| **CNN-FE** | 89.00 | 92.00 | 89.00 | 90.41 | 0.892 | 278.5 | 94.3 |
| **TRANSFER LEARNING** | 89.20 | 93.00 | 90.40 | 92.50 | 0.916 | 165.6 | 51.9 |
| **Fine-tuning** | 91.40 | 97.40 | 93.20 | 94.37 | 0.968 | 132.7 | 35.4 |

The performance of three deep learning models CNN-FE, transfer learning, and fine-tuning is shown in Table 9 in terms of precision, recall, f1-score, accuracy, and kappa value. CNN-FE exhibited a commendable performance with a precision of 89.00%, recall of 92.00%, F1-score of 89.00%, accuracy of 90.41%, and a kappa value of 0.892. These metrics collectively indicate a strong ability of CNN-FE to correctly classify within the dataset, balancing both precision and recall effectively. Transitioning to transfer learning, the model exhibited slightly improved performance across most metrics. With a precision of 89.20%, recall of 93.00%, F1-score of 90.40%, accuracy of 92.50%, and a kappa value of 0.916%, transfer learning showcased enhanced accuracy beyond that of CNN-FE. This transfer learning model used the pre-existing knowledge effectively, refining classification capabilities and increasing overall model performance. Finally, fine-tuning outperformed both CNN-FE and transfer learning, exhibiting superior precision (91.40%), recall (97.40%), F1-score (93.20%), accuracy (94.37%), and a notably high kappa value of 0.968. These results highlight the effectiveness of fine-tuning in LULC classification, resulting in significantly improved performance across all evaluated metrics.

The computation training and testing times of three deep learning models CNN-FE, transfer learning, and fine-tuning is also shown in Table 9. The CNN-FE demonstrated a training time of 278.5 seconds and a testing time of 94.3 seconds. Transfer learning, on the other hand, was more efficient, requiring only 165.6 seconds for training and 51.9 seconds for testing. Finally, the fine-tuning approach showed the fastest performance with a training time of 132.7 seconds and a testing time of 35.4 seconds. These results highlight the varying computational demands of each method, with fine-tuning proving to be the most time-efficient.

## 6.2. Comparison of State-of-the-art Methods

The comparative analysis of the proposed CNN-based DL models with existing classifiers demonstrates the effectiveness of our approach when applied to the LISS-III dataset. Unlike many previous works that reported results on different datasets such as Sentinel-2, Landsat-8, or other high-resolution imagery, in this study we have implemented the models developed by various researchers and evaluated them uniformly on the same LISS-III dataset. This ensures a fair and controlled comparison, eliminating biases arising from differences in spatial resolution, sensor characteristics, and study regions.

As shown in Table 10, the three proposed models CNN-FE, TL, and FT consistently outperformed conventional classifiers. Among these, the fine-tuning approach achieved the highest accuracy of 94.37% with a Kappa value of 0.968, significantly higher than traditional classifiers such as k-NN (87.28%), Decision Trees (83.24%), SVM (86.71%), MLC (85.42%), and RF (88.93%). This demonstrates the superiority of deep learning methods in extracting complex spatial–spectral features from medium-resolution imagery.

When compared with CNN architectures reported in earlier studies (Benyamin Hosseiny et al. 2022, Jingtao et al. 2020, and Bryan Sencaki et al. 2023), the proposed fine-tuned CNN showed notable improvements.

Jingtao et al. (2020) achieved 92.65% accuracy, while our fine-tuned model reached 94.37% on the same dataset. Similarly, the transfer learning model in this work achieved 92.50% accuracy, validating the adaptability of pretrained networks to LISS-III data. These comparisons highlight that the proposed models not only generalize well but also enhance performance when benchmarked under identical experimental conditions.

It is also important to note that while many prior studies reported promising accuracies, their results were based on higher-resolution datasets, making direct comparison with medium-resolution LISS-III data scientifically weak. In contrast, by applying these models directly on our LISS-III dataset, we ensure a methodologically correct and reliable comparison. This approach confirms that with proper model adaptation, LISS-III imagery can achieve classification accuracies that are on par with, or even surpass, results obtained from higher-resolution datasets.

Finally, the consistently higher Kappa values obtained in this study, particularly for the fine-tuned CNN (0.968), underline the reliability of our model by reducing the likelihood of chance agreement. This indicates not only higher overall accuracy but also stronger class-level agreement, which is crucial for LULC mapping.

In summary, the results clearly establish that our proposed CNN-based DL models especially the fine-tuned variant are better suited for LULC classification using LISS-III data than both traditional classifiers and existing CNN implementations by other researchers. By conducting controlled, dataset-consistent comparisons, this work demonstrates that medium-resolution Indian remote sensing imagery can be effectively utilized for high-accuracy land use monitoring when advanced DL techniques are employed.

**Table 10.** Proposed CNN-based DL model comparison with existing classifiers

| **#** | **Proposed DL models** | | | **Benyamin Hosseiny et al (2022)** | **García-Gutiérrez et al. (2010)** | **Narimane Zaabar et al. (2022)** | **Milap Punia et al. (2011)** | **Jingtao et al. (2020),** | **Bryan Sencaki et al. (2023)** | **Zerrouki N et al.(2019)** | **Mandla Dlamini et al. (2021)** | **GN Vivekananda et al. (2021)** | **Chaitanya (2022)** |
|---|---|---|---|---|---|---|---|---|---|---|---|---|---|
| **Classifier** | **CNN-FE** | **TF** | **Fine-tunning** | **CNN** | **k-NN** | **CNN** | **DT** | **CNN** | **CNN** | **WRF** | **SVM** | **MLC** | **RF** |
| **Accuracy(%)** | 90.41 | 92.50 | 94.37 | 92.74 | 87.28 | 92.65 | 83.24 | 91.24 | 90.62 | 86.15 | 86.71 | 85.42 | 88.93 |
| **Kappa Value** | 0.892 | 0.916 | 0.968 | 0.901 | 0.845 | 0.912 | 0.824 | 0.904 | 0.894 | 0.874 | 0.846 | 0.832 | 0.861 |

## 6. CONCLUSIONS

This research paper presented deep learning models to enhance the accuracy of LULC classification. CNN-FE model was designed and trained from scratch, transfer learning and fine-tuning models were trained from the pre-existing model. The deep learning model's performance was examined in terms of various performance metrics such as precision, recall, F1-score, accuracy, and kappa value. The experiment results show that fine-tuning exhibited the highest performance across all metrics, with precision, recall, F1-score, and accuracy reaching impressive values of 91.40%, 97.40%, 93.20%, and 94.37% respectively. Transfer learning also demonstrated notable performance, closely following fine-tuning with precision, recall, F1-score, and accuracy of 89.20%, 93.00%, 90.40%, and 92.50% respectively. CNN-FE, while slightly lagging behind transfer learning and fine-tuning, still showcased acceptable results with precision, recall, F1-score, and accuracy at 89.00%, 92.00%, 89.00%, and 90.41% respectively. These findings have practical implications for various applications, including urban planning, environmental monitoring, and natural resource management, where precise LULC classification is imperative for informed decision-making and sustainable development.

**Author Contributions:** For research articles with multiple authors, include a brief paragraph outlining each author's contributions using the following format: "Conceptualization, Mahendra H N.; methodology, Mahendra H N.; software, Mahendra H N.; validation, Basavaraju N M., Ravi P. and Pushpalatha V.; formal analysis, Maendra H N, Mallikarjunaswamy S.; investigation, Mahendra H N.; resources, Mahendra H N.; data curation, Mahhendra H N, Basavaraju N M.; writing—original draft preparation, Mahendra H N; writing—review and editing, Mahendra H N, Basavaraju N M, and Pushapalatha V.; visualization, Mahendra H N.; supervision, Mahendra H N, Mallikarjunaswamy S; project administration, Mahendra H N, and Basavaraju N M. All authors have read and agreed to the published version of the manuscript. Authorship should be restricted to individuals who have made significant contributions to the research.

**Funding:** This research work was financially supported through the seed money funding provided by JSS Academy of Technical Education, Bengaluru. The funding enabled access to computational resources, data processing facilities, and necessary tools required to successfully carry out the study. No additional external funding was received for this research.

**Acknowledgments:** We would like to thank JSS Academy of technical Education Bengaluru and NRSC, ISRO for providing the satellite data for the research work.

**Conflicts of Interest:** The author declares that there are no conflicts of interest regarding the subject matter of this research article.

## REFERENCES

Alem, A., & Kumar, S. (2021). Transfer Learning Models for Land Cover and Land Use Classification in Remote Sensing Image. Applied Artificial Intelligence, 36(1). https://doi.org/10.1080/08839514.2021.2014192.

Abdi, Abdulhakim. (2019). Land cover and land use classification performance of machine learning algorithms in a boreal landscape using Sentinel-2 data. GIScience & Remote Sensing. 57. 1-20. 10.1080/15481603.2019.1650447.

Agarwal, Rashi & Goel, Silky & Nijhawan, Rahul. (2022). Using Deep Learning Approach for Land-Use and Land-Cover Classification based on Satellite images. 1-8. 10.1109/ASIANCON55314.2022.9909395.

Alem, Abebaw & Kumar, Shailender. (2020). Deep Learning Methods for Land Cover and Land Use Classification in Remote Sensing: A Review. 903-908. 10.1109/ICRITO48877.2020.9197824.

Alhassan, Victor & Henry, Christopher J. & Ramanna, Sheela & Storie, Christopher. (2020). A deep learning framework for land-use/land-cover mapping and analysis using multispectral satellite imagery. Neural Computing and Applications. 32. 10.1007/s00521-019-04349-9.

Balarabe, Anas & Jordanov, Ivan. (2021). LULC Image Classification with Convolutional Neural Network. 5985-5988. 10.1109/IGARSS47720.2021.9555015.

Bergado, John Ray & Persello, Claudio & Stein, Alfred. (2020). LAND USE CLASSIFICATION USING DEEP MULTITASK NETWORKS. ISPRS - International Archives of the Photogrammetry, Remote Sensing and Spatial Information Sciences. XLIII-B3-2020. 17-21. 10.5194/isprs-archives-XLIII-B3-2020-17-2020.

Bryan Sencaki, D, Mega Novetrishka Putri, Budi Heru Santosa, Siti Arfah, Robby Arifandri, Afifuddin, Muhammad Iqbal Habibie, Prabu Kresna Putra, Nico Anatoly, Zilda Dona Okta Permata, Marina C.G. Frederik, Agustan, Lena Sumargana, Hari Priyadi, (2023). Land cover multiclass classification of wonosobo, Indonesia with time series-based one-dimensional deep learning model, Remote Sensing Applications: Society and Environment, Volume 32, 2023.https://doi.org/10.1016/j.rsase.2023.101040.

Boyang Li; Weihua Su; Hang Wu; Ruihao Li; Wenchang Zhang; Wei Qin; Shiyue Zhang., (2020). "Further Exploring Convolutional Neural Networks' Potential for Land-Use Scene Classification," in IEEE Geoscience and Remote Sensing Letters, vol. 17, no. 10, pp. 1687-1691, Oct. 2020, doi: 10.1109/LGRS.2019.2952660.

Carranza-García, Manuel & García-Gutiérrez, Jorge & Riquelme, José. (2019). A Framework for Evaluating Land Use and Land Cover Classification Using Convolutional Neural Networks. Remote Sensing. 11. 274. 10.3390/rs11030274.

Census reports of India. https://censusindia.gov.in/census.website/.

Chaitanya B. Pande., 2022. Land use/land cover and change detection mapping in Rahuri watershed area (MS), India using the google earth engine and machine learning approach, Geocarto International, DOI: 10.1080/10106049.2022.2086622.

Dewangkoro, H & Arymurthy, Aniati. (2021). Land Use and Land Cover Classification Using CNN, SVM, and Channel Squeeze & Spatial Excitation Block. IOP Conference Series: Earth and Environmental Science. 704. 012048. 10.1088/1755-1315/704/1/012048.

Douass, S., & Ait Kbir, M. (2022). Deep learning approach for land use images classification. E3S Web of Conferences. https://doi.org/10.1051/e3sconf/202235101043

E. Maggiori, Y. Tarabalka, G. Charpiat and P. Alliez, "Convolutional Neural Networks for Large-Scale Remote-Sensing Image Classification," in IEEE Transactions on Geoscience and Remote Sensing, vol. 55, no. 2, pp. 645-657, Feb. 2017, doi: 10.1109/TGRS.2016.2612821.

Fahmi, Hisyam & Sari, Wina. (2022). Analysis of deep learning architecture for patch-based land cover classification. 1-5. 10.1109/ICITISEE57756.2022.10057895.

García-Gutiérrez, Jorge & Mateos-García, Daniel & Riquelme, José. (2010). A SVM and k-NN Restricted Stacking to Improve Land Use and Land Cover Classification. 493-500. 10.1007/978-3-642-13803-4_61.

Geetha & Gowda, Karegowda & Rudrappa, Nandeesha & Nagaraj, B. (2021). Change Detection of LULC using Machine Learning. 10.2991/ahis.k.210913.042.

Gibril, Mohamed & Abu Bakar, Suzana Binti & Yao, KOUAME & Mohammed, & Idrees, Mohammed & Pradhan, Biswajeet. (2016). Fusion of RADARSAT 2 and multispectral optical remote sensing data for LULC extraction in a tropical agricultural area. Geocarto International. 32. 10.1080/10106049.2016.1170893.

Gisela Häufel, Lukas Lucks, Melanie Pohl, Dimitri Bulatov, Hendrik Schilling, "Evaluation of CNNs for land cover classification in high-resolution airborne images," Proc. SPIE 10790, Earth Resources and Environmental Remote Sensing/GIS Applications IX, 1079003 (9 October 2018); https://doi.org/10.1117/12.2325604

GN Vivekananda, R Swathi & AVLN Sujith., (2021). Multi-temporal image analysis for LULC classification and change detection, European Journal of Remote Sensing, 54:sup2, 189-199, DOI: 10.1080/22797254.2020.1771215.

Henry, Christopher J. & Storie, Christopher & Alagappan, Muthu Palaniappan & Alhassan, Victor & Swamy, Mallikarjun & Aleshinloye, Damilola & Curtis, Andrew & Kim, Daeyoun. (2019). Automated LULC map production using deep neural networks. International Journal of Remote Sensing. 40. 1-25. 10.1080/01431161.2018.1563840.

Haikel Alhichri, & Alsuwayed, Asma & Bazi, Yakoub & Ammour, Nassim & Alajlan, Naif. (2021). Classification of Remote Sensing Images Using EfficientNet-B3 CNN Model with Attention. IEEE Access. PP. 1-1. 10.1109/ACCESS.2021.3051085.

Hosseiny, B., Abdi, A. M., & Jamali, S. (2022). Urban land use and land cover classification with interpretable machine learning – A case study using Sentinel-2 and auxiliary data. Remote Sensing Applications: Society and Environment, 28, Article 100843. https://doi.org/10.1016/j.rsase.2022.100843.

Jingtao Yao, Tarik Mitran, Xiangbin Kong, Rattan Lal, Qing Chu & Muhammad Shaukat., 2020. Landuse and land cover identification and disaggregating socio-economic data with convolutional neural network, Geocarto International, 35:10, 1109-1123, DOI: 10.1080/10106049.2019.1568587.

Kalantar, Bahareh & Seydi, Seyd & Ueda, Naonori & Saeidi, Vahideh & Abdul Halin, Alfian & Shabani, Farzin. (2022). Deep Ensemble Learning for Land Cover Classification Based on Hyperspectral Prisma Image. 3612-3615. 10.1109/IGARSS46834.2022.9884203.

K. Ganesha Raj, Shivam Trivedi, K. S. Ramesh, R. Sudha, S. Rama Subramoniam, H. M. Ravishankar, A. Vidya., 2020, Assessment of Vegetation Cover of Bengaluru City, India, Using Geospatial Techniques. J Indian Soc Remote Sens 49, 747–758 (2021). https://doi.org/10.1007/s12524-020-01259-5.

Kumar, Saurabh & Arya, Shwetank. (2021). Change Detection Techniques for Land Cover Change Analysis Using Spatial Datasets: a Review. Remote Sensing in Earth Systems Sciences. 4. 10.1007/s41976-021-00056-z.

Kussul, Nataliia & Lavreniuk, Mykola & Skakun, Sergii & Shelestov, Andrey. (2017). Deep Learning Classification of Land Cover and Crop Types Using Remote Sensing Data. IEEE Geoscience and Remote Sensing Letters. PP. 1-5. 10.1109/LGRS.2017.2681128.

Li, Boyang & Su, Weihua & Wu, Hang & Li, Ruihao & Zhang, Wenchang & Qin, Wei & Zhang, Shiyue & Wei, Jiacheng. (2019). Further Exploring Convolutional Neural Networks' Potential for Land-Use Scene Classification. IEEE Geoscience and Remote Sensing Letters. PP. 1-5. 10.1109/LGRS.2019.2952660.

Liang H, Li Q. (2016) Hyperspectral Imagery Classification Using Sparse Representations of Convolutional Neural Network Features. Remote Sensing 8(2):99. https://doi.org/10.3390/rs8020099.

Liu, Bo & Du, Shihong & Zhang, Xiuyuan. (2020). Land Cover Classification Using Convolutional Neural Network with Remote Sensing Data And Digital Surface Model. ISPRS Annals of Photogrammetry, Remote Sensing and Spatial Information Sciences. V-3-2020. 39-43. 10.5194/isprs-annals-V-3-2020-39-2020.

Mozumder, S., Parveen, M. and Pasha, A.K., 2025. Changes in Land Use Land Cover and its Resultant Impacts on the Urban Thermal Environment of Chattogram City: A Spatio-Temporal Analysis Based on Remote Sensing and GIS Techniques. Nature Environment and Pollution Technology, 24(2), pp.1-15. 10.46488/NEPT.2025.v24i02.D1714

Mahendra, H. N., Pushpalatha, V., Rekha, V., Sharmila, N., Mahesh Kumar, D., Pavithra, G. S., ... & Mallikarjunaswamy, S. (2025). Land Use/Land Cover (LULC) Change Classification for Change Detection Analysis of Remotely Sensed Data Using Machine Learning-Based Random Forest Classifier. Nature Environment & Pollution Technology, 24(2), pp. 1-10. https://doi.org/10.46488/NEPT.2025.v24i02.B4238.

Mahendra, H.N, Mallikarjunaswamy, S. and S Rama Subramoniam.., 2023a. An assessment of vegetation cover of Mysuru City, Karnataka State, India, using deep convolutional neural networks, Environmental Monitoring Assessment, 195, 526. https://doi.org/10.1007/s10661-023-11140-w.

Mahendra H.N, Mallikarjunaswamy, S, and Sudalayandi Rama Subramoniam,2023b, An assessment of built-up cover using geospatial techniques – a case study on Mysuru district, Karnataka state, India", Int. J. Environmental Technology and Management,. DOIhttp://dx.doi.org/10.1504/IJETM.2022.10048734.

Mahendra H.N, and Mallikarjunaswamy, S, 2023c, An analysis of change detection in land use land cover area of remotely sensed data using supervised classifier", International Journal of Environmental Technology and Management, Oct 2023 Vol.26. DOI: 10.1504/IJETM.2023.134322

Mahendra, H. N., & Mallikarjunaswamy, S. (2022). "An Efficient Classification of Hyperspectral Remotely Sensed Data Using Support Vector Machine," International Journal of Electronics and Telecommunications, 68(3), 609-617. DOI: 10.24425/IJET.2022.141280.

Mandla Dlamini, Elhadi Adam, George Chirima & Hamisai Hamandawana., 2021. A remote sensing-based approach to investigate changes in land use and land cover in the lower uMfolozi floodplain system, South Africa, Transactions of the Royal Society of South Africa, 76:1, 13-25, DOI: 10.1080/0035919X.2020.1858365.

Milap Punia, P.K. Joshi, M.C. Porwal, Decision tree classification of land use land cover for Delhi, India using IRS-P6 AWiFS data, Expert Systems with Applications, Volume 38, Issue 5, 2011, Pages 5577-5583, https://doi.org/10.1016/j.eswa.2010.10.078.

M. Tan and Q. V. Le, ``EfficientNet: Rethinking model scaling for convolutional neural networks,'' 2019, arXiv:1905.11946.

Naushad, R., Kaur, T., & Ghaderpour, E. (2021). Deep Transfer learning for Land Use and Land Cover Classification: A Comparative Study. Sensors (Basel, Switzerland), 21. https://doi.org/10.3390/s21238083

National portal of India. https://www.india.gov.in/india-glance/profile

Nijhawan, Rahul & Joshi, Deepankar & Narang, Naman & Mittal, Aditya & Mittal, Ankush. (2019). A Futuristic Deep Learning Framework Approach for Land Use-Land Cover Classification Using Remote Sensing Imagery. 10.1007/978-981-13-0680-8_9.

N. Zaabar, S. Niculescu and M. M. Kamel, 2022. Application of Convolutional Neural Networks With Object-Based Image Analysis for Land Cover and Land Use Mapping in Coastal Areas: A Case Study in Ain Témouchent, Algeria, in IEEE Journal of Selected Topics in Applied Earth Observations and Remote Sensing, vol. 15, pp. 5177-5189. doi: 10.1109/JSTARS.2022.3185185.

Patel, Sanskruti & Ganatra, Nilay & Patel, Rachana. (2022). Multi-level Feature Extraction for Automated Land Cover Classification using Deep CNN with Long Short-Term Memory Network. 1123-1128. 10.1109/ICOEI53556.2022.9777148.

Pushpalatha, V., Mahendra, H. N., Prasad, A. M., Sharmila, N., Kumar, D. M., Basavaraju, N. M., ... & Mallikarjunaswamy, S. (2024). An Assessment of Land Use Land Cover Using Machine Learning Technique. Nature Environment and Pollution Technology, 23(4), pp. 2211-2219. https://doi.org/10.46488/NEPT.2024.v23i04.025.

Rao, Duvvada & Noorjahan, Shaik & Fathima, Shaik. (2022). Classification of Land Cover Usage from Satellite Images using Deep Learning Algorithms. 1302-1308. 10.1109/ICEARS53579.2022.9752282.

Ram Kumar Singh, Prafull Singh, Martin Drews, Pavan Kumar, Hukum Singh, Ajay Kumar Gupta, Himanshu Govil, Amarjeet Kaur, Manoj Kumar,2021. A machine learning-based classification of LANDSAT images to map land use and land cover of India, Remote Sensing Applications: Society and Environment, Volume 24. https://doi.org/10.1016/j.rsase.2021.100624.

Sathyanarayanan, Dinesh & Anudeep, DV & Das, C & Bhandarkar, Sanat & Damotharan, Uma & Ram, Hebbar & Kasar-agod, Ganesha Raj. (2020). A Multiclass Deep Learning Approach for LULC Classification of Multispectral Satellite Images. 102-105. 10.1109/InGARSS48198.2020.9358947.

Shabbir, Amsa & Ali, Nouman & Jameel, Ahmed & Zafar, Bushra & Rasheed, Aqsa & Sajid, Muhammad & Ahmed, Afzal & Dar, Saadat. (2021). Satellite and Scene Image Classification Based on Transfer Learning and Fine Tuning of ResNet50. Mathematical Problems in Engineering. 2021. 10.1155/2021/5843816.

Shihab, Tay & Al-Hameedawi, Amjed & Hamza, Ammar. (2020). Random Forest (RF) and Artificial Neural Network (ANN) Algorithms for LULC Mapping. Engineering and Technology Journal. 38. 510-514. 10.30684/etj.v38i4A.399.

Sivamalar, P. & Preetha, S & Banu, E & Madhumitha, S & Sindhiya, R. (2023). An Enhanced Remote Sensing Image Classification for LC/LU using Deep Convolutional Neural Networks. 1560-1566. 10.1109/ICSCDS56580.2023.10104896.

Song, Yang & Zhang, Zhifei & Kaviani Baghbaderani, Razieh & Wang, Fanqi & Qu, Ying & Stuttsy, Craig & Qi, Hairong. (2019). Land Cover Classification for Satellite Images Through 1D CNN. 1-5. 10.1109/WHISPERS.2019.8921180.

Sudhakar Sengan, Arodh Lal Karn, Denis A. Pustokhin, Irina V. Pustokhina, Meshal Alharbi, 2022. A hybrid learning model for efficient classification of Land Use and land change from satellite images, Physics and Chemistry of the Earth, Parts A/B/C, Volume 128. https://doi.org/10.1016/j.pce.2022.103284.

Uba, N.K. (2019). Land Use and Land Cover Classification Using Deep Learning Techniques. ArXiv, abs/1905.00510.

Wang, Aili & He, Xin & Ghamisi, Pedram & Chen, Yushi. (2018). LiDAR Data Classification Using Morphological Profiles and Convolutional Neural Networks. IEEE Geoscience and Remote Sensing Letters. PP. 1-5. 10.1109/LGRS.2018.2810276.

Wang M, Zhang H, Sun W, Li S, Wang F, Yang G., 2020. A Coarse-to-Fine Deep Learning Based Land Use Change Detection Method for High-Resolution Remote Sensing Images. Remote Sensing. 12(12):1933. https://doi.org/10.3390/rs12121933.

Weng, Qian & Mao, Zhengyuan & Lin, Jiawen & Guo, Wenzhong. (2017). Land-Use Classification via Extreme Learning Classifier Based on Deep Convolutional Features. IEEE Geoscience and Remote Sensing Letters. PP. 1-5. 10.1109/LGRS.2017.2672643.

Weng, Qian & Mao, Zhengyuan & Lin, Jiawen & Liao, Xiangwen. (2018). Land-use scene classification based on a CNN using a constrained extreme learning machine. International Journal of Remote Sensing. 39. 1-19. 10.1080/01431161.2018.1458346.

World Bank data, 2022. https://data.worldbank.org/indicator/AG.LND.ARBL.ZS?locations=IN

Xia, Bin & Kong, Fanyu & Zhou, Jun & Wu, Xin & Xie, Qiong. (2022). Land Resource Use Classification Using Deep Learning in Ecological Remote Sensing Images. Computational Intelligence and Neuroscience. 2022. 1-9. 10.1155/2022/7179477.

Xin-Yi Tong, Gui-Song Xia, Qikai Lu, Huanfeng Shen, Shengyang Li, Shucheng You, Liangpei Zhang., 2020. Land-cover classification with high-resolution remote sensing images using transferable deep models, Remote Sensing of Environment, Volume 237. https://doi.org/10.1016/j.rse.2019.111322.

Yang, Chun & Rottensteiner, Franz & Heipke, Christian. (2018). CLASSIFICATION OF LAND COVER AND LAND USE BASED ON CONVOLUTIONAL NEURAL NETWORKS. ISPRS Annals of Photogrammetry, Remote Sensing and Spatial Information Sciences. IV-3. 251-258. 10.5194/isprs-annals-IV-3-251-2018.

Yang, Chun & Rottensteiner, Franz & Heipke, Christian. (2021). A hierarchical deep learning framework for the consistent classification of land use objects in geospatial databases. 10.48550/arXiv.2104.06991.

Yang, Bin & hu, Shunshi & Guo, Qiandong & Hong, Danfeng. (2022). Multi-Source Domain Transfer Learning Based on Spectral Projections for Hyperspectral Image Classification. IEEE Journal of Selected Topics in Applied Earth Observations and Remote Sensing. 15. 1-1. 10.1109/JSTARS.2022.3173676.

Yang, Xuan & Chen, Zhengchao & Bp, Li & Peng, Dailiang & Chen, Pan. (2019). A Fast and Precise Method for Large-Scale Land-Use Mapping Based on Deep Learning. 5913-5916. 10.1109/IGARSS.2019.8898705.

Yao, Jingtao & Mitran, Tarik & Kong, Xiangbin & Lal, Rattan & Chu, Qing & Shaukat, Muhammad. (2019). Landuse and land cover identification and disaggregating socio-economic data with convolutional neural network. Geocarto International. 1-13. 10.1080/10106049.2019.1568587.

Zerrouki, N., Harrou, F., Sun, Y., & Hocini, L., 2019. A Machine Learning-Based Approach for Land Cover Change Detection Using Remote Sensing and Radiometric Measurements. IEEE Sensors Journal, 19(14), 5843–5850. doi:10.1109/jsen.2019.2904137.

Zhang, C., Sargent, I., Pan, X., Li, H., Gardiner, A., Hare, J.S., & Atkinson, P.M. (2019). Joint Deep Learning for land cover and land use classification. Remote Sensing of Environment. https://doi.org/10.1016/j.rse.2018.11.014.

Zhu, M. & Wu, B. & He, Y. & He, Y.. (2020). Land Cover Classification Using High Resolution Satellite Image Based On Deep Learning. ISPRS - International Archives of the Photogrammetry, Remote Sensing and Spatial Information Sciences. XLII-3/W10. 685-690. 10.5194/isprs-archives-XLII-3-W10-685-2020.